Electronic Supplementary Material (ESI) for Analyst.

Multifunctional Exo III-assisted Scalability Strategy for Constructing DNA Molecular Logic Circuits

(Supplementary Information)

Chenyi Zeng,†[a] Xin Liu,†[b] Bin Wang,[a] Rui Qin,[a] Qiang Zhang*[a]

a. Key Laboratory of Advanced Design and Intelligent Computing, Ministry of Education, School of Software Engineering, Dalian University, Dalian 116622, China. Email: zccc9802@163.com(C.Z.); wangbin@dlu.edu.cn(B.W.); qinrui9850@163.com (R.Q.); zhangq@dlu.edu.cn(Q.Z.)

b. School of Computer Science and Technology, Dalian University of Technology, Dalian 116024, China. xinliuaisky@mail.dlut.edu.cn(X.L.)

† These authors contribute equally to this work.

* Correspondence: zhangq@dlu.edu.cn; Tel.: +86-0411-87402106

Contents

Table S1. Synthetic oligonucleotide sequences

Sequence	from 5' to 3'
S1Up	GTTCAGATGGTTCATGTATCTTCAGTGTGTGCTAGTGGATG T*T*T*T*T
S1Dn	CATCCACTAGCACACACTGAAGATACATGCAGACTAGAGT CT*T*T*T*T
Z1	GACTCTAGTCTGCATGTATC/idSp/TCAGTGTGTGCTAGTGG ATGT*T*T*T*T
A*	ATCAGTGTGTGCTAGTGGATGC*A*G*T*T
R1Up	5`6-FAM CAGTTCAGATGGTTCAT*T*T*T*T
R1Dn	GATACATGAACCATCTGAAC/iBHQ1dT/GT*T*T*T*T
R2Up	5`ROX TGCAGACTAGAGTCTCT*T*T*T*T
R2Dn	GAGACTCTAGTCTGCATGTA/iBHQ2dT/CT*T*T*T*T
S2Up	5`ROX CAAGTTCAAGTGGTTCAGATGGTTT*T*T*T*T
S2Dn	GATACATGAACCATCTGAACCACTTGAACT/iBHQ2dT/GCC ATCCAGT*T*T*T*T
S3Up	5`6-FAM CAGACTAGAGTCCTGATGT*T*T*T*T
S3Dn	AGGACTCTAGTC/iBHQ1dT/GCATGTATCTCAGTGTGTGCTA GTGGATGT*T*T*T*T
S4Up	CAGACTAGAGTCCTGATACCGTACT*T*T*T*T
S4Dn	CGCTAAGTGTACGGTATCAGGACTCTAGTCTGCATGTATCT *T*T*T*T
Z2	CTGGATGGCAAGTTCAAGTGT*T*T*T*T
Z3	CTGATACCGTACACTTAGCGT*T*T*T*T

S2. Verification of non-specific hydrolysis resistance

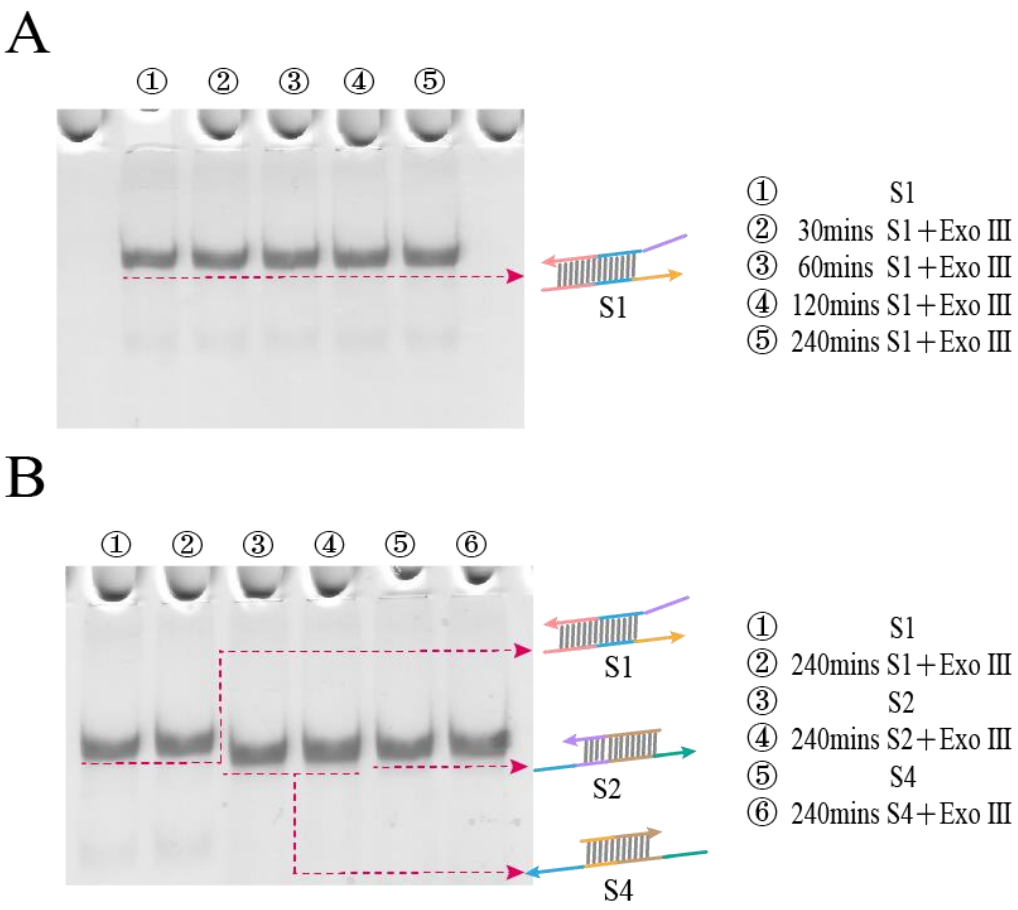

Fig S2 (A) Gel electrophoresis of substrate S1 with Exo III for different times. Lane 1, S1; lane 2, 30mins S1 + Exo III; lane 3, 60mins S1 + Exo III; lane 4, 120mins S1 + Exo III; lane 5, 240mins S1 + Exo III. (B) Gel electrophoresis of different substrates coexisting with Exo III. Lane 1, S1; lane 2, 240mins S1 + Exo III; lane 3, S2; lane 4, 240mins S2 + Exo III; lane 5, S4; lane 6, 240mins S4 + Exo III. [S1] = [S2] = [S4] = 20 pmol, Exo III = 4 U.

To avoid non-specific hydrolysis by Exo III, we performed anti-hydrolysis experiments of several substrates. We tested the resistance of non-specific hydrolysis for different durations of the same substrate S1 (Fig S2. A) and for same durations of different substrates (Fig S2. B). All substrates, exemplified by S1, S2 and S4, overcome non-specific hydrolysis well and could co-exist with Exo III in solution.

S3. Re-hybridization between V1 and V2

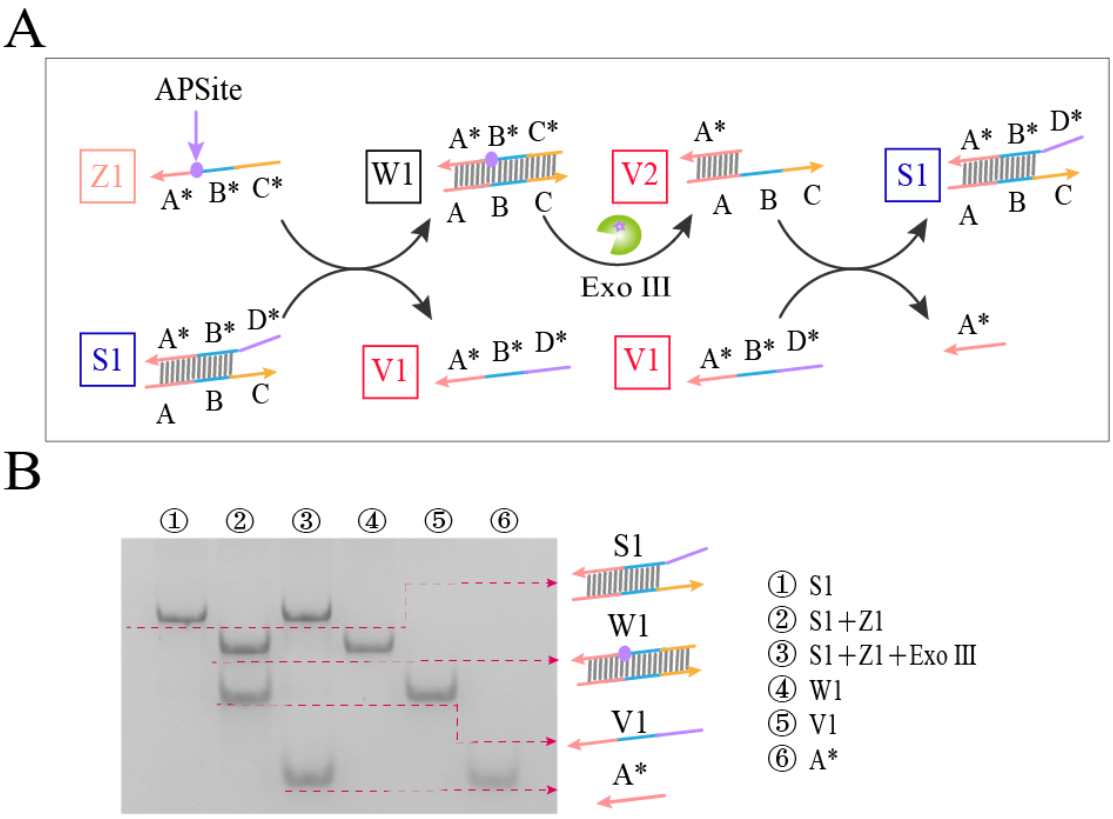

Fig S3 (A) Schematic diagram of re-hybridization between V1 and V2. (B) Gel electrophoresis of re-hybridization between V1 and V2. Lane 1, S1; lane 2, S1 + Z1; lane 3, S1 + Z1 + Exo III; lane 4, W1; lane 5, V1; lane 6, A*.

The re-hybridization of signals V1 and V2 during activation of the signaling pathway was the primary cause of signal loss, as shown in Fig. S3A. Z1 occurred once strand displacement reaction with substrate S1. The Exo III hydrolyzed the double-stranded DNA with an AP site to expose the available toehold domain and activated an additional signal V2. However, the signals V1 and V2 regenerated S1 when signal V1 or V2 was unable to react with downstream signals. The re-hybridization hindered the activation of both signaling pathways.

We verified the re-hybridization between V1 and V2 by polyacrylamide gel electrophoresis experiments in Fig. S3B. In the absence of Exo III, the single-stranded DNA with an AP site occurred once strand displacement reaction with substrate S1 in lane 2. The strand displacement reaction only activated output signal V1. In the presence of Exo III, Exo III hydrolyzed waste W1 to additional output V2. However, the re-hybridization occurred between signals V1 and V2 when signal V1 or V2 was unable to react with downstream signals. Signal V1 and V2 re-generated substrate S1 by strand displacement reaction in lane 3.

S4. The influence of concentrations of Exo III on signal transmission

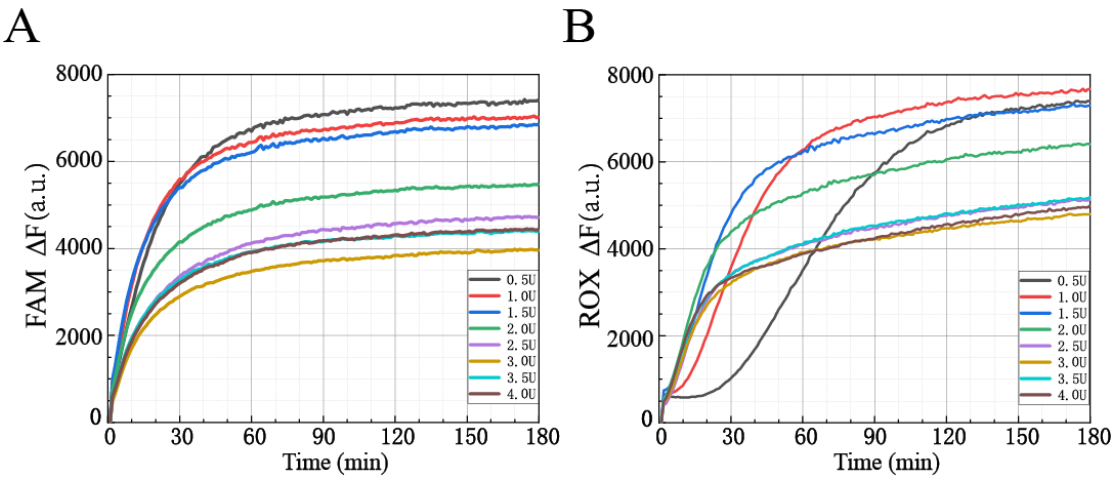

Fig S4 (A) Fluorescence kinetic traces of different concentrations of Exo III in the FAM channel. (B) Fluorescence kinetic traces of different concentrations of Exo III in the ROX channel. The fluorescence values in the graphs were averaged over three sets of experiments and multiplexed.

The real-time fluorescence traces of different concentrations of Exo III were shown in Fig. S4. Exo III is highly catalytic, and low concentrations of Exo III could even hydrolysis fast. For the DSS strategy, a suitable hydrolysis rate could effectively avoid signal loss. The fluorescence values decreased gradually as the concentration of Exo III increased. When Exo III is in the range of 0.5–4 U, there was an obvious signal loss from 2 U. For the range of 0.5–1.5 U, the fluorescence traces showed similar reaction rates in the FAM channel. On the other hand, the fluorescence traces showed different reaction rates in the ROX channel. When Exo III was 0.5 U, the reaction rate was significantly slower than the 1 U and 1.5 U cases in the ROX channel. There were the highest fluorescence values when Exo III was 1 U. The experimental data showed that the fluorescence value of fan-out circuit had an inverse correlation with the concentrations of Exo III. Overall, 1 U Exo III was chosen for further study.

S5. Signal performance with different concentration of S1 in fan-out circuit

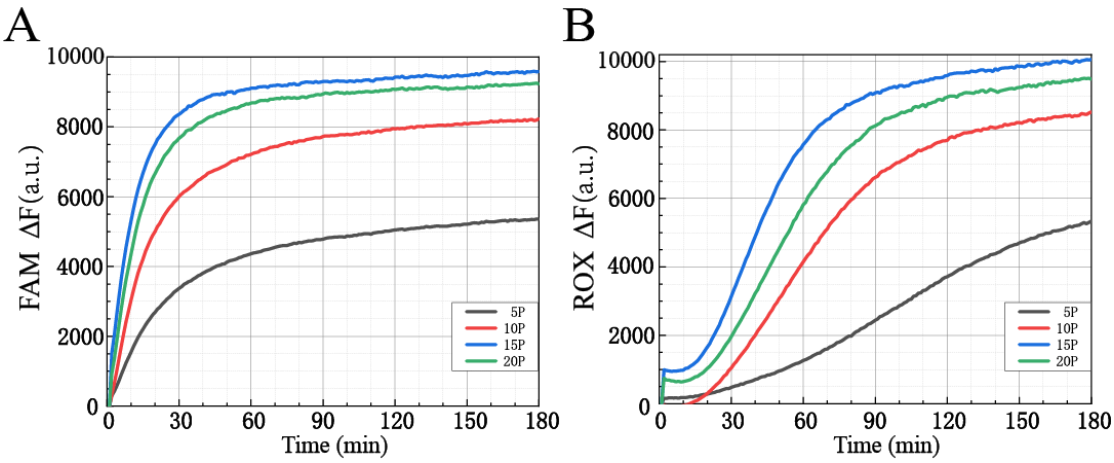

Fig S5 (A) Fluorescence kinetic traces of different concentrations of S1 in the FAM channel. (B) Fluorescence kinetic traces of different concentrations of S1 in the ROX channel. The fluorescence values in the graphs were averaged over three sets of experiments and multiplexed.

A higher concentration of S1 could produce sufficient output signals, decreasing signal leakage. The real-time fluorescence traces of different concentrations of S1 were shown in Fig. S5. As shown in the kinetic traces, we fixed Z1 at 20 pmol. When S1 increased from 5 to 15 pmol, both the amount of fluorescence change and the reaction rate increased effectively. When S1 was 20 pmol, reaction rate did not continue to increase due to the limited hydrolysis capacity of 1U Exo III. Overall, 15 pmol S1 was chosen for further study.

S6. Signal performance with different concentration of Z1 in fan-out circuit

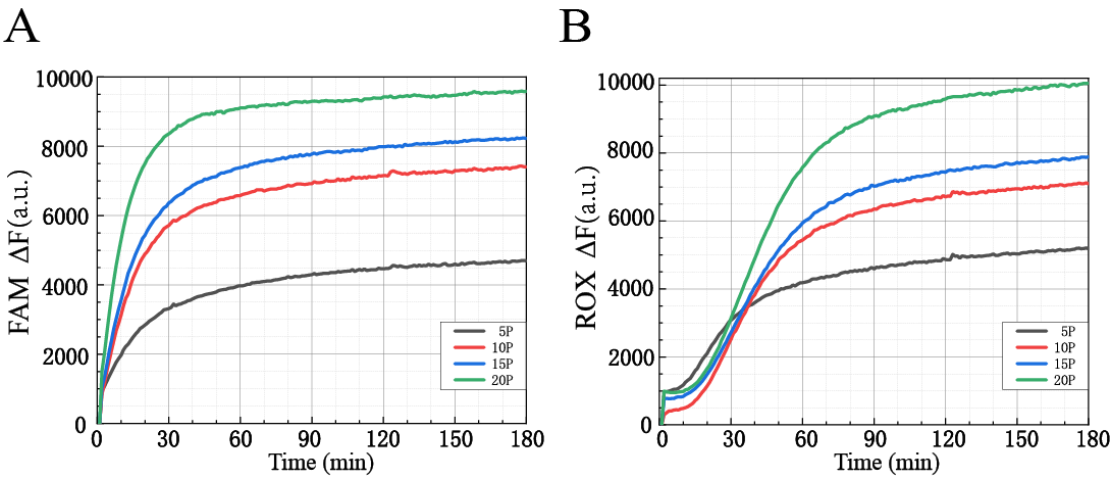

Fig S6 (A) Fluorescence kinetic traces of different concentrations of Z1 in the FAM channel. (B) Fluorescence kinetic traces of different concentrations of Z1 in the FAM channel. The fluorescence values in the graphs were averaged over three sets of experiments and multiplexed.

A higher concentration of Z1 could promote strand displacement reaction, increasing reaction rate. The real-time fluorescence traces of different concentrations of Z1 were shown in Fig. S6. As shown in the kinetic traces, we fixed S1 at 15 pmol. The amount of fluorescence change and the rate of reaction were significantly increased as Z1 gradually increased. The experimental data showed that the reaction rate of fan-out circuit had a positive correlation with the concentrations of Z1. Overall, 20 pmol Z1 was chosen for further study.

S7. Signal performance with different concentration of Z2 in cascade circuits

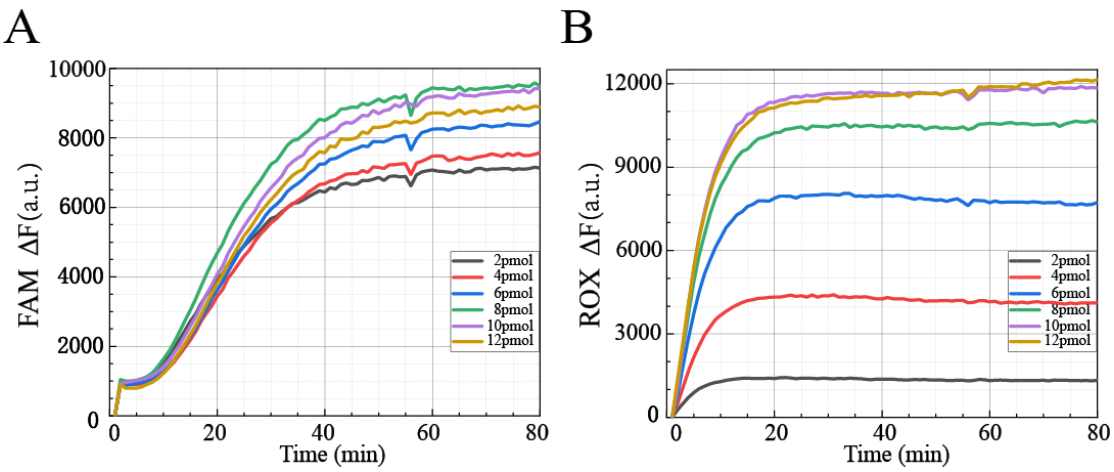

Fig S7 (A) Fluorescence kinetic traces of different concentrations of Z2 in the FAM channel. (B) Fluorescence kinetic traces of different concentrations of Z2 in the FAM channel

For cascaded circuits, concentrations of other input strands influenced the performance of logic functions. The real-time fluorescence traces of different concentrations of Z2 are referred Fig. S7. For the range of 2–10 pmol, the fluorescence traces showed progressive increase of reaction rates in the FAM channel as concentrations of Z2 increase. The amount of fluorescence increased with the amount of input Z2 in the ROX channel. The concentration of the input Z2 also facilitated the signal transmission. However, there was no obvious difference when Z2 was more than 10 pmol. The experimental result indicates that 10 pmol Z2 is the optimum condition for further study.

S8. A double-logic cascade circuit with parallel AND and AND logic functions

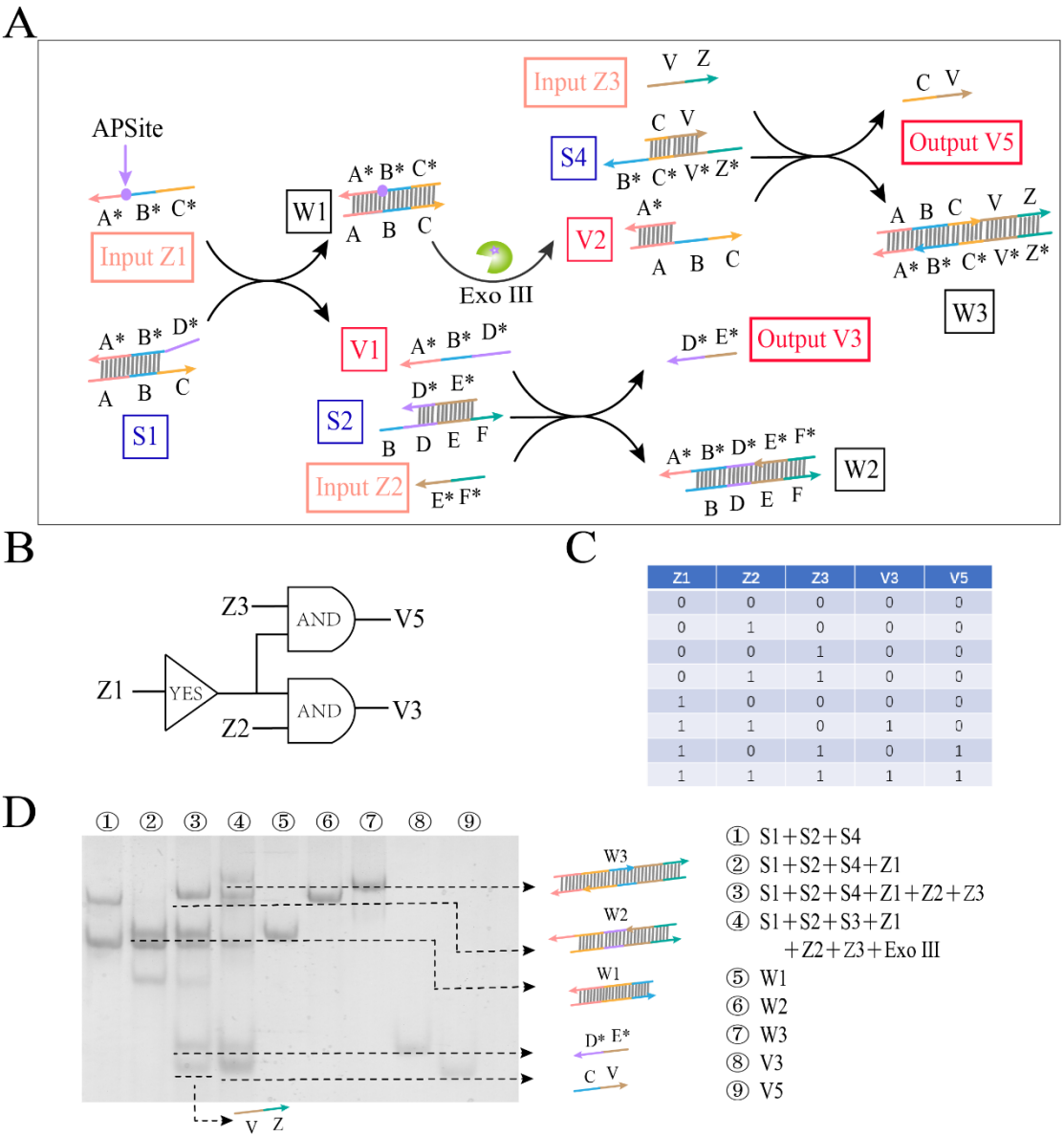

Fig S8. (A) Schematic diagram of the double-logic AND-AND cascade circuit driven by Exo III. The circuit consists of three substrates and Exo III. The input signals are Z1, Z2 and Z3. The output signals are V3 and V5. (B) The cascade circuit symbol. (C) The truth table. (D) Polyacrylamide gel electrophoresis illustration of cascade circuit. Lane 1, S1 + S2 + S4; lane 2, S1 + S2 + S4 + Z1; lane 3, S1 + S2 + S3 + Z1 + Z2 + Z3; lane 4, S1 + S2 + S3 + Z1 + Z2 + Z3 + Exo III; lane 5, W1; lane 6, W2; lane 7, W3; lane 8, V3; lane 9, V5. [Z1] = [Z2] = [Z3] = [S1] = [S2] = [S4] = 20 pmol，Exo = 1 U.

To demonstrate multiple logical computing capabilities, a double-logic cascade

circuit with parallel AND and AND logic functions was constructed, as shown in S8. The entire cascade circuit included two substrates S1, S2 and S4. The symbols for the cascaded circuit were shown in S8. B. The truth table was shown in S8. C.

We verified the feasibility of this logic circuit by polyacrylamide gel, as shown in S8.D. In the absence of Exo III, input Z1 only completed strand displacement reaction to produce strand V1. But the V1 could not complete the strand displacement reaction for AND gate alone and no output was produced. In the presence of two inputs Z1, Z2 and Z3, two double-stranded waste and output strand V3 were obtained by two strand displacement reactions. In the presence of Exo III, the three inputs Z1, Z2 and Z3 produced two different signal outputs. Based on the illustration of polypropylene gel electrophoresis, we successfully verified the feasibility of a double-logic cascade circuit with parallel AND and AND logic functions and it met the expected experimental results.